Amphitheater-headed canyons formed by megaflooding at Malad Gorge, Idaho

Michael P. Lamb[1], Benjamin H. Mackey[2], and Kenneth A. Farley

Division of Geological and Planetary Sciences, California Institute of Technology, Pasadena, CA 91125

Edited by Thure E. Cerling, University of Utah, Salt Lake City, UT, and approved November 25, 2013 (received for review June 27, 2013)

Many bedrock canyons on Earth and Mars were eroded by upstream propagating headwalls, and a prominent goal in geomorphology and planetary science is to determine formation processes from canyon morphology. A diagnostic link between process and form remains highly controversial, however, and field investigations that isolate controls on canyon morphology are needed. Here we investigate the origin of Malad Gorge, Idaho, a canyon system cut into basalt with three remarkably distinct heads: two with amphitheater headwalls and the third housing the active Wood River and ending in a 7% grade knickzone. Scoured rims of the headwalls, relict plunge pools, sediment-transport constraints, and cosmogenic (^{3}He) exposure ages indicate formation of the amphitheater-headed canyons by large-scale flooding ∼46 ka, coeval with formation of Box Canyon 18 km to the south as well as the eruption of McKinney Butte Basalt, suggesting widespread canyon formation following lava-flow diversion of the paleo-Wood River. Exposure ages within the knickzone-headed canyon indicate progressive upstream younging of strath terraces and a knickzone propagation rate of 2.5 cm/y over at least the past 33 ka. Results point to a potential diagnostic link between vertical amphitheater headwalls in basalt and rapid erosion during megaflooding due to the onset of block toppling, rather than previous interpretations of seepage erosion, with implications for quantifying the early hydrosphere of Mars.

megaflood | knickpoint | sapping | waterfall

Landscapes adjust to perturbations in tectonics and base level through upstream propagation of steepened river reaches, or knickzones, thereby communicating environmental signals throughout a drainage basin (e.g., ref. 1). Nowhere are knickzones more important and apparent than in landscapes where canyon heads actively cut into plateaus, such as tributaries of the Grand Canyon, United States, and the basaltic plains of Mars (e.g., refs. 2–4). Here the stark topographic contrast between low-relief uplands and deeply incised canyons sharply delineates canyon rims and planform morphology. Canyon heads can have varied shapes from amphitheaters with vertical headwalls to more pointed planform shapes with lower gradients, and a prominent goal in geomorphology and planetary science is to link canyon morphology to formation processes (e.g., refs. 4–8), with implications for understanding the history of water on Mars.

Amphitheater-headed canyons on Mars are most likely cut into layered basalt (9, 10), and canyon-formation interpretations have ranged widely from slow seepage erosion to catastrophic megafloods (4–6, 11, 12). Few studies have been conducted on the formation of amphitheater-headed canyons in basalt on Earth, however, and instead, terrestrial canyons in other substrates are often used as Martian analogs. For example, groundwater sapping is a key process in forming amphitheater-headed canyons in unconsolidated sand (e.g., refs. 8, 13, 14), but its importance is controversial in rock (5, 12, 15). Amphitheater-headed canyons are also common to plateaus with strong-over-weak sedimentary rocks (3, 16); however, here the tendency for undercutting is so strong that canyon-head morphology may bear little information about erosional processes, whether driven by groundwater or overland flow (e.g., refs. 3, 5, 17). Canyons in some basaltic landscapes lack strong-over-weak stratigraphy, contain large boulders that require transport, and show potential for headwall retreat by block toppling (18–21), all of which make extension of process–form relationships in sand and sedimentary rocks to basalt and Mars uncertain.

To test the hypothesis of a link between canyon formation and canyon morphology in basalt, we need field measurements that can constrain formation processes for canyons with distinct morphologies, but carved into the same rock type. Here we report on the origin of Malad Gorge, a canyon complex eroded into columnar basalt with markedly different shaped canyon heads. Results point to a potential diagnostic link between canyon-head morphology and formative process by megaflood erosion in basalt.

Malad Gorge is a tributary to the Snake River Canyon, Idaho, within the Snake River Plain, a broad depression filled by volcanic flows that erupted between ∼15 Ma and ∼2 ka (22, 23). The gorge sits at the northern extent of Hagerman Valley, a particularly wide (∼7 km) part of the Snake River Canyon (Fig. 1). Malad Gorge is eroded into the Gooding Butte Basalt [^{40}Ar/^{39}Ar eruption age: 373 ± 12 ka (25)] which is composed of stacked lava beds, each several meters thick with similar well-defined columns bounded by cooling joints and no apparent differences in strength between beds. The Wood (or Malad) River, a major drainage system from the Sawtooth Range to the north, drains through Malad Gorge before joining the Snake River. The Wood River is thought to have been diverted from an ancestral, now pillow lava-filled canyon into Malad Gorge by McKinney Butte basalt flows (24) [^{40}Ar/^{39}Ar eruption age: 52 ± 24 ka (25) (Fig. 1).

Malad Gorge contains three distinct canyon heads herein referred to as Woody's Cove, Stubby Canyon, and Pointed Canyon (Fig. 2*A*). Woody's Cove and Stubby have amphitheater heads with ∼50-m-high vertical headwalls (Fig. 2*C*), and talus accumulation at headwall bases indicates long-lived inactive fluvial

Significance

The shapes of bedrock canyons offer clues to the history of surface water on Earth and Mars. Using field examples in Idaho, we found that canyons with amphitheater-shaped heads were likely carved rapidly by outburst flooding about 46,000 y ago and that canyons with more pointed heads evolved progressively by river erosion over tens of thousands of years. Our study suggests that the many amphitheater-headed canyons in fractured basalt on Mars, long inferred to be carved by groundwater seepage, may owe their origins instead to megafloods.

Author contributions: M.P.L. and B.H.M. designed research; M.P.L. and B.H.M. performed research; K.A.F. contributed new reagents/analytic tools; M.P.L., B.H.M., and K.A.F. analyzed data; and M.P.L., B.H.M., and K.A.F. wrote the paper.

The authors declare no conflict of interest.

This article is a PNAS Direct Submission.

[1]To whom correspondence should be addressed. E-mail: mpl@gps.caltech.edu.

[2]Present address: Department of Geological Sciences, University of Canterbury, Christchurch, New Zealand.

This article contains supporting information online at www.pnas.org/lookup/suppl/doi:10.1073/pnas.1312251111/-/DCSupplemental.

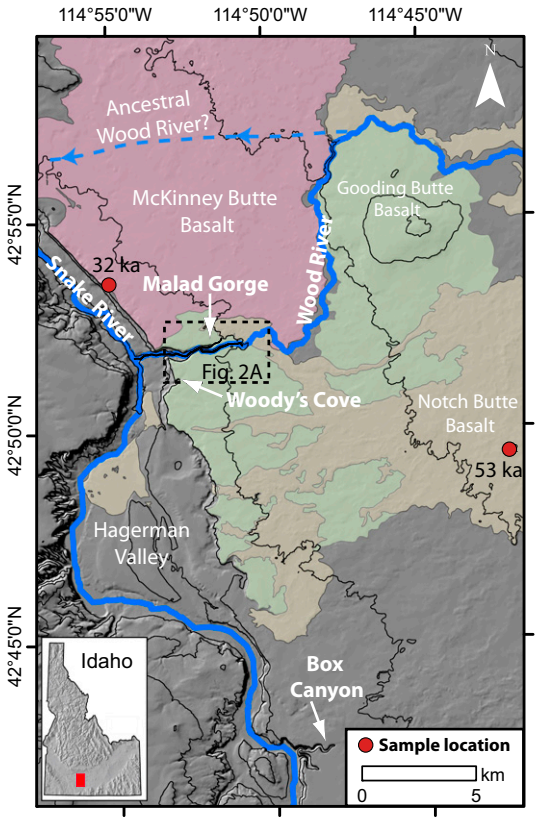

Fig. 1. Shaded relief map of the study region (50-m contour interval) showing basalt flows (23), their exposure age sample locations, and the path of the ancestral Wood River following Malde (24) (US Geological Survey).

transport (Fig. 3 *A* and *B*). Woody's Cove, the shortest of the three canyons, lacks major spring flows and has minor, intermittent overland flow partially fed by irrigation runoff that spills over the canyon rim. Stubby has no modern-day overland flow entering the canyon, and springs emanate from a pool near its headwall (Fig. 3*B*). In contrast, Pointed Canyon is distinctly more acute in planform morphology, contains a 7% grade knickzone composed of multiple steps rather than a vertical headwall (Figs. 2*C* and 3*C*), and extends the farthest upstream.

Early work attributed the amphitheater-headed canyons in this region—Malad Gorge, Box Canyon, located 18 km south of Malad Gorge (Fig. 1), and Blue Lakes Canyon located 42 km to the SE—to formation by seepage erosion because of no modern overland flow and the occurrence of some of the largest springs in the United States in this region (7). Because spring flows (e.g., ~10 m^3/s in Box Canyon; US Geological Survey gauge 13095500) are far deficient to move the boulders that line the canyon floors, Stearns (7) reasoned that the boulders must chemically erode in place. This explanation is improbable, however, given the young age of the Quaternary basalt (25), spring water saturated in dissolved solids (19), and no evidence of rapid chemical weathering (e.g., talus blocks are angular and have little to no weathering rinds). Instead of groundwater sapping, Box Canyon was likely carved by a large-scale flood event that occurred ~45 ka based on ^{3}He cosmogenic exposure age dating of the scoured rim of the canyon headwall (19, 26). In addition, Blue Lakes Canyon was formed during the Bonneville Flood [~18–22 ka (27, 28)], one of the world's largest outburst floods that occurred as a result of catastrophic draining of glacial lake Bonneville (21). In both cases, canyon formation was inferred to have occurred through upstream headwall propagation by waterfall erosion.

Herein we aim to test whether the amphitheater-headed canyons at Malad Gorge also owe their origin to catastrophic flooding, whether Pointed Canyon has a different origin, and whether canyon morphology is diagnostic of formation process. To this end we present field observations, sediment-size measurements, hydraulic modeling, and cosmogenic exposure ages of water-scoured rock surfaces and basalt-flow surfaces (*Methods* and Tables S1 and S2).

Results

We inspected the canyon rims and the escarpment that separates Woody's Cove from the rest of Malad Gorge and mapped scoured rock as indications of overland flow. Scours consist of linear abrasion marks (flutes), often millimeters in depth and centimeters long, that fan outward in the inferred downstream flow direction (Fig. S1). The amphitheater-headed canyons at Malad Gorge have scoured rock upstream indicating overland flow in the past (Fig. 2). Both amphitheater-headed canyons have notches cut into their headwalls showing evidence for plucking (missing blocks) and abrasion (polished and fluted rock surfaces). For example, the notch at the head of Stubby Canyon is ~10 m deep with respect to the neighboring basaltic plain and cuts basalt-flow stratigraphy (Fig. 3*D*). In addition, both amphitheater-headed canyons have large pools at their heads (e.g., Fig. 3*B*), similar to plunge pools at the base of waterfalls. The pool at Stubby Canyon, for example, is ~120 m in diameter (Fig. 4*A*) and partially filled with sediment. Canyon headwalls are vertical and not undercut (Fig. 3 *A* and *B*), and the bedrock is blocky and jointed suggesting canyon-head erosion by block plucking and toppling (18, 29). The bedrock scours upstream of the canyon heads, scoured notches at the canyon-head rims, vertical and blocky canyon headwalls, and large relict plunge pools at Malad Gorge canyons are similar to features found at Box Canyon and Blue Lakes Canyon, evidence used at those sites and elsewhere to support canyon formation by large-scale flooding (e.g., refs. 19–21, 30).

We collected samples of polished bedrock surfaces from the notches of the amphitheater-headed canyons for cosmogenic ^{3}He exposure age dating (*Methods* and Tables S1 and S2). In both cases, eroded notches are sufficiently deep (10 m for Stubby Canyon and 2.6 m for Woody's Cove) that any inherited cosmogenic exposure before erosion is negligible. The exposure age at the rim of Woody's Cove is 47 ± 3 ka, which is within error of the oldest of three samples taken from the rim of Stubby (46 ± 3 ka). These ages are also within error of the age of the notch cut into the rim of Box Canyon [45 ± 5 ka (26)]. The other four samples of scoured rock within Stubby Canyon cluster with an average of 20.6 ± 2.6 ka (Table S2), coincident with upper age constraints for the Bonneville Flood (27, 28). Together, these exposure ages indicate the formation of all three amphitheater-headed canyons in this region (Box Canyon, Woody's Cove, and Stubby Canyon) may have been coeval, ceasing ~46 ka, except for later reworking during backwater inundation by the Bonneville Flood.

To constrain the discharge necessary to mobilize the boulders that line the canyon floors, which is a necessary condition for canyon formation, we measured sediment sizes and surveyed channel dimensions within Stubby Canyon (at GS1 in Fig. 2*B*; *Methods*). Median particle diameters are 0.58 m with the largest boulders exceeding 3 m (Fig. 4*B*). The river-bed gradient downstream of the plunge pool has a near-constant slope of 0.0043 (Fig. 4*A*), and modern spring-fed water depths average 1.0 m (Fig. 4*C*). These data were used as inputs into hydraulic resistance and incipient sediment motion formulas (*Methods*) to find a modern spring discharge of 11 m^3/s [similar to measurements within Box Canyon (19)] and a paleoflood necessary to mobilize the boulder bed that has a calculated minimum discharge of 1,250 m^3/s and a minimum water depth of 9 m (Fig. 4*C*). Large paleodischarges are also inferred from boulder bars (median grain diameter of 0.32 m; Fig. 4*B*) upstream of the canyon (GS2 in Fig. 2*B*) where the flood was largely unconfined.

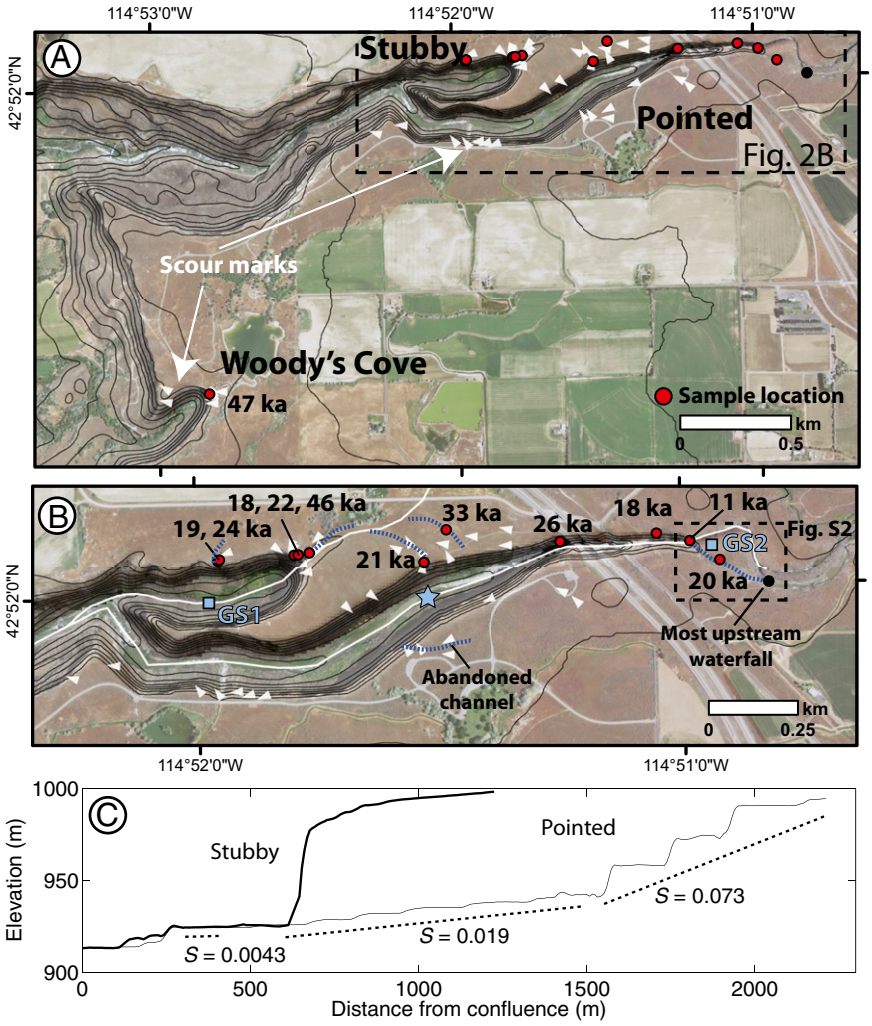

Fig. 2. Malad Gorge topography (10-m contour interval) and aerial orthophotography (US Geological Survey). (*A*) Overview map and (*B*) close-up for Stubby and Pointed canyons showing mapped bedrock scours (white arrows), exposure age sample locations (red circles) with age results, location of the uppermost active knickpoint (black circle), abandoned bedrock channels (blue dashed lines), and grain-size analysis sites (blue squares). The blue star shows the reconstructed location of the headwall of Pointed Canyon at 46 ka (see *Discussion* and Fig. 5). (*C*) Longitudinal profile along Stubby and Pointed canyons from their confluence (shown as white lines in *B*) with local slope, *S*, averaged over regions demarked by dashed lines (Fig. 4*A* shows close-up of profile in Stubby Canyon).

The calculated minimum canyon-forming discharge is approximately sevenfold the largest historic discharge of the Wood River (181 m^3/s over a 98-y record; US Geological Survey gauge 13152500) and more than 100-fold the calculated modern spring discharge, indicating that the flood(s) that carved the amphitheater-headed canyons of Malad Gorge were extraordinary. Our discharge estimate is consistent with calculated flow depths of 2–6 m needed to exceed the threshold for megaflood erosion by block toppling in this region (18). Moreover, it is similar to the discharge calculated for the canyon-carving flood at Box Canyon [800–2,800 m^3/s (19)] and far smaller than discharge calculated for the Bonneville Flood [10^6 m^3/s (30)].

In contrast to the two amphitheater-headed canyons at Malad Gorge, the third canyon ends in an active knickzone that houses the Wood River (Fig. 3*C*) and contains abundant markers of active fluvial abrasion (rather than block toppling), most notably, nested potholes (Fig. 3*E*). At the upstream extent of the knickzone, the active channel narrows from ∼20 to ∼1 m in width as water plunges into the gorge and abandons the pothole-laden river bed at its margins as a strath terrace (Fig. 3*E*). Similar strath terraces abut both sides of Pointed Canyon along its upper ∼1 km. Upstream of Malad Gorge, the Wood River is anabranching, and the propagation of the uppermost knickpoint appears to have pirated water that once flowed into a neighboring channel (Fig. S2). The abandoned channel contains abundant potholes and a now-dry waterfall (Fig. 3*F*). Additional abandoned channels exist farther downstream on both sides of Pointed Canyon (Fig. 2*B*), and abrasion marks within the channels indicate flow into Pointed Canyon in some cases and out of Pointed Canyon in other cases, supporting progressive abandonment of anabranches due to knickzone propagation.

To test whether Pointed Canyon was formed by progressive knickzone retreat, we collected samples for exposure age dating from strath terraces and abandoned channels (Fig. 2*B*, *Methods*, and Tables S1 and S2). Three of the resulting dates fall within the age range of the Bonneville Flood, and because the Bonneville Flood likely inundated Malad Gorge in full (30), reworking and erosion of even the uppermost terraces cannot be ruled out. The other exposure ages show progressive younging in the upstream direction (Fig. 5) with a ∼33-ka abandoned channel at x = 1,300 m (where x is the distance from the confluence of Pointed and Stubby canyons), to an 11-ka abandoned channel at x = 1,900 m, to the most upstream extent of the knickzone where terrace abandonment is active (Fig. S2 and Fig. 3*E*). These ages suggest, over at least the past 33 ka, a constant rate of knickzone retreat of 2.5 cm/y (by linear regression, r^2 = 0.99), and a constant rate is expected given that 1 km of retreat has not affected the 7,800 km^2 drainage area to the knickpoint (e.g., refs. 1, 2). It is possible that the Bonneville Flood partially affected all of the exposure ages in Pointed Canyon, but this cannot explain the 11 ka age that is younger than the flood, nor the linear, upstream-younging trend in ages that intersects the modern knickpoint location at ∼0 ka (Fig. 5). Moreover, flood erosion, where it

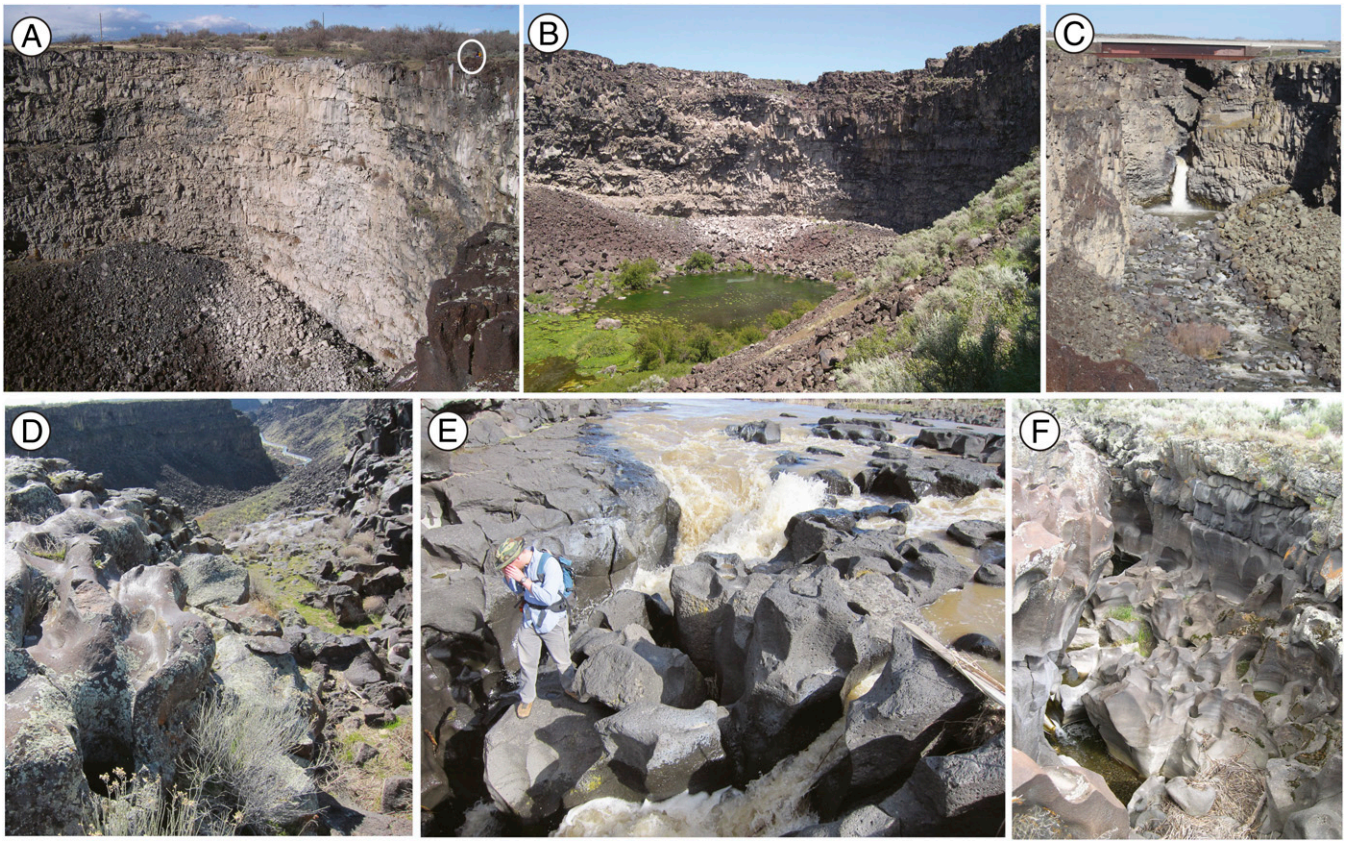

Fig. 3. Photographs of (*A*) headwall of Woody's Cove (person for scale, circled), (*B*) ~50-m-high headwall of Stubby Canyon, (*C*) downstream-most waterfall at Pointed Canyon knickzone (12-m-high waterfall with overcrossing highway for scale), (*D*) fluted and polished notch at the rim of Stubby Canyon (notch relief is 10 m), (*E*) upstream-most waterfall at Pointed Canyon knickzone (within the southern anabranch of Fig. S2), and (*F*) upstream-most abandoned channel in Fig. 2*B* and Fig. S2 (channel relief is ~10 m). White coloring on the headwalls in *A* and *B* is likely residue from irrigation runoff.

occurred, likely completely reset ages owing to plucking of meter-scale blocks.

Discussion

Scoured rock, eroded notches into canyon-head rims, plunge pools, sediment-transport constraints, and cosmogenic exposure ages suggest that the amphitheater-headed canyons of Malad Gorge were carved by large-scale flooding that ceased ~46 ka, and similar data from Box Canyon (19, 26) suggest a common origin. Exposure ages of the canyon heads are similar to the eruption age of the McKinney Butte Basalt [$^{40}Ar/^{39}Ar$ age of 52 ± 24 ka (25)], and independent evidence that the Wood River was diverted to its present course at this time (24) suggests a causal connection between diversion of the Wood River and the incision of Malad Gorge and Box Canyon. This hypothesis is consistent with the onset of a regional loess deposit [~40 ka (31)] that does not show flood scour and must postdate flooding, in addition to the surface exposure age we measured for Notch Butte Basalt (^{3}He age of 52.8 ± 3.4 ka; *Methods* and Tables S1 and S2), which is largely loess free, crosscut by the Wood River just upstream of the knickzone, and must predate river diversion (Fig. 1). To improve age constraints for McKinney Butte Basalt, we measured an ^{3}He exposure age of the flow surface of 31.9 ± 1.9 ka (Fig. 1, *Methods*, and Tables S1 and S2); however, this age is necessarily a minimum eruption age due to abundance of loess cover here (23) and potential for erosion of the original flow surface (32). Still, we cannot rule out the possibility that the Wood River diversion postdates formation of the amphitheater-headed canyons, in which case an alternative flood source such as a glacial lake outburst (e.g., refs. 19, 33, 34) from the Sawtooth Range must be invoked.

The similar timing of the McKinney Butte basalt flows and the cessation of flooding recorded by exposure ages on the canyon rims suggests that flooding was short-lived and possibly a single event. Given that the necessary discharge for canyon cutting far exceeds historical floods of the Wood River, we suggest lava flows must have dammed the Wood River resulting in outburst flooding where sheets of flood water focused locally to erode distinct amphitheater-headed canyons. These floods may also have eroded the eastern wall of the Snake River canyon between Malad Gorge and Box Canyon resulting in the anomalously wide Hagerman Valley (Fig. 1). Furthermore, a short-duration flood event explains why there is little landscape dissection upstream of the canyon heads; in the absence of an unbuttressed escarpment, block toppling is not possible (18, 29), and the floods must have been limited to the comparatively slow processes of fluvial abrasion and localized plucking, which require thousands of years or more for channelization (1).

Once volcanism at McKinney Butte ceased, we infer that the Wood River established its modern path to Pointed Canyon and abandoned the amphitheater-headed canyons. Given the measured knickzone retreat rates of 2.5 cm/y in Pointed Canyon, our interpretation implies that Pointed Canyon was ~1 km long at the cessation of megaflooding (Fig. 5), placing the ancestral canyon head near the location where the modern-day canyon begins to taper in width (blue star in Fig. 2*B*). Therefore, Pointed Canyon may have been partly carved by megaflooding and may once have had an amphitheater head, perhaps similar to the branching amphitheater-headed canyons on Mars (4). Since the

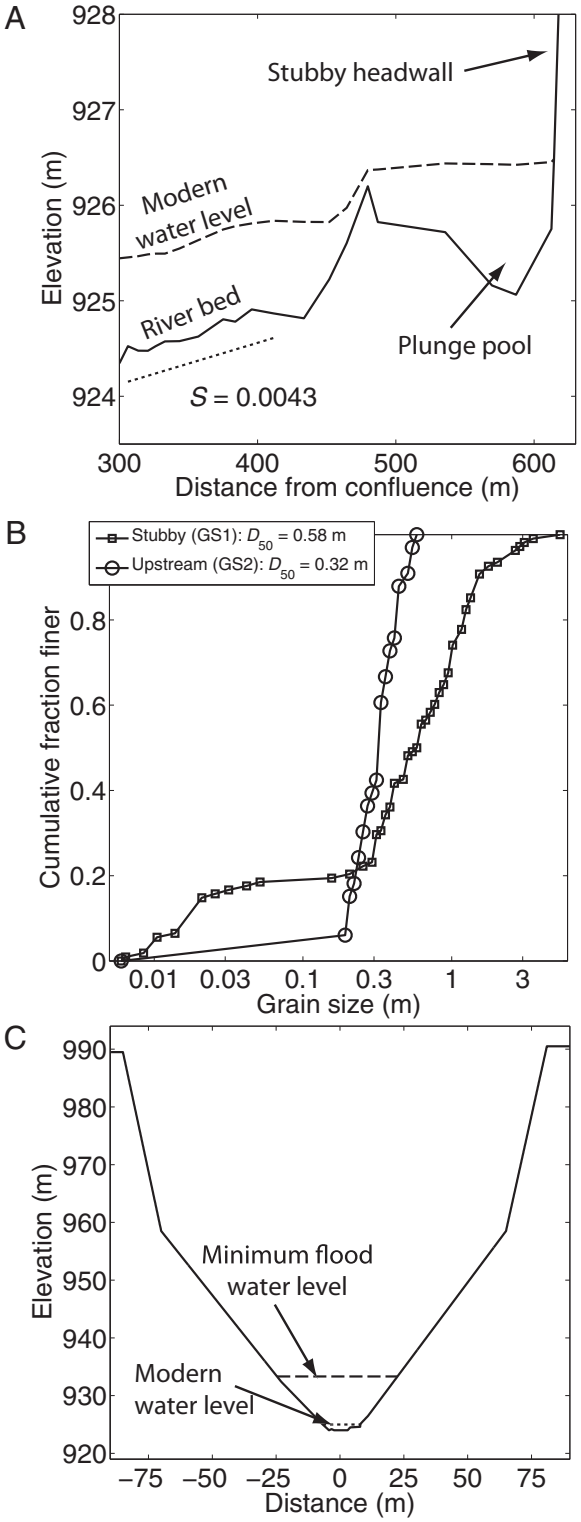

Fig. 4. (A) Thalweg long profile of the head of Stubby Canyon showing the modern (spring-driven) water level. The region of the river bed downstream of the plunge pool ($S = 0.0043$) was used for hydraulic calculations. (*B*) Sediment-size distributions within the survey location of Stubby Canyon (GS1 in Fig. 2*B*; 113 counts) and of a boulder bar upstream of the canyons (GS2 in Fig. 2*B*; 32 counts). The median sediment size (D_{50}) at location GS1 was used for calculations (*Methods*). (*C*) Surveyed canyon cross-section of Stubby Canyon at GS1 (Fig. 2*B*) showing the flood depth calculated to move the bouldery bed (*Methods*) and the modern flow depth. The break in slope at 958-m elevation represents the transition from bedrock walls above to talus below.

cessation of megaflooding, the comparatively low discharges of the Wood River do not exceed the threshold for block toppling, leaving only the steady upstream propagation of the pointed headwall by fluvial abrasion.

Our study suggests that amphitheater-headed canyons with vertical walls in columnar basalt may be a diagnostic indicator of rapid megaflood erosion rather than persistent fluvial abrasion or seepage erosion. The rationale for this hypothesis is that *i*) basalt with vertical cooling joints and horizontal bedding planes tends to break down to large, meter-sized boulders that cannot be transported by seepage alone; *ii*) vertically jointed rock promotes persistent vertical headwalls and rapid erosion if a threshold discharge for block toppling is surpassed, which in turn requires high-magnitude overland flows (18); and *iii*) the overland flow events must be of short duration, otherwise fluvial abrasion will tend to flatten the headwall and dissect the upstream landscape, as shown in Pointed Canyon. There are a host of canyons cut into columnar basalt by megafloods that support our hypothesis: Asbyrgi Canyon in Iceland (35), canyons cut by the Missoula Floods (20), Blue Lakes Canyon and Devil's Corral cut by the Bonneville Flood (21, 28, 30), and Box Canyon (19).

Many of these terrestrial amphitheater-headed canyons in basalt appear morphologically similar to putative cataracts in outflow channels and valley networks with amphitheater heads on Mars (e.g., refs. 4, 6, 12). Given confirmation of columnar basalt (e.g., ref. 10) and canyon heads that lack well-developed undercuts, Martian canyons with amphitheater heads may also owe their origin to short-lived, high-magnitude flood events, possibly sourced from subsurface water eruptions, dam-burst floods, or lake spillover (e.g., ref. 36). Most landscape evolution models applied to Earth and Mars do not include jointed rock or erosion by toppling and consequently only produce amphitheater-headed canyons by using rules for seepage erosion in sand (e.g., refs. 8, 15, 37). In contrast, in basalt the onset of toppling may be the tipping point to form amphitheater-headed canyons,

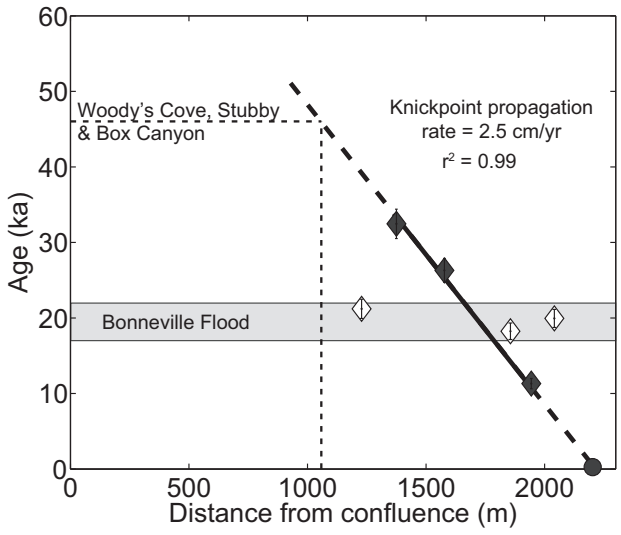

Fig. 5. Exposure age versus distance projected along the long profile (Fig. 2*C*) of Pointed Canyon. Three samples (open symbols) yielded ages consistent with reworking by the Bonneville Flood and are not included in the fit (note one of the three falls nearly on the trend line). Error bars represent analytical uncertainty (Table S2), which is often smaller than the symbol size. The most upstream age of zero (filled circle) is assumed based on the observed location of active knickzone retreat (Fig. 3*E* and Fig. S2). Data suggest Pointed Canyon was 1.05 km long (blue star in Fig. 2*B*) when formation of the other canyons ceased (~46 ka). The Bonneville Flood age range shown extends a few thousand years older than is typically reported based on revised chronology of paleoshorelines (27) and canyon exposure ages (28).

which implies drastically different water discharges and flow durations for canyon formation than groundwater sapping.

Methods

Fourteen rock samples were taken for ^{3}He cosmogenic exposure-age dating: five from Stubby Canyon, six from Pointed Canyon, one from Woody's Cove, one from McKinney Butte Basalt, and one from Notch Butte Basalt (Figs. 1 and 2 and Tables S1 and S2). A cosmic ray-shielded sample used to correct all canyon erosion samples (BG0 in Table S1) was taken from 5.8 m deep within a crack located ~4 m from the canyon sidewall of Pointed Canyon. The crack splits a viewing platform indicating it has opened historically. Shielded samples for McKinney Butte and Notch Butte basalts were taken from road cuts (MB0 and NB0 in Table S2).

Samples were collected by chipping off the upper 4 cm of rock on near-horizontal surfaces. We separated 250- to 450-μm-diameter olivine and pyroxene grains from the crushed host rock by standard magnetic, heavy liquid, and hand picking techniques. Adhering groundmass was removed by sonicating samples in 5% (vol/vol) 2:1 HF:HNO3 acid for ~1 h. Samples were ground and wet-sieved to <37 microns which largely removes mantle-derived ^{3}He trapped in melt and/or fluid inclusions (38). The remaining matrix-sited ^{3}He and ^{4}He was measured on a MAP 215-50 noble gas mass spectrometer following heating to 1,300 °C in vacuum to release the gas (39) (Table S1). Shielded samples were used to correct for remaining mantle-derived and nucleogenic ^{3}He (40), which only averaged 6% of the total measured ^{3}He (Table S1). Accumulation ages and production rates (Tables S1 and S2) were calculated using the Lifton/Sato scaling scheme (41, 42) on the CRONOS ^{3}He calculator (43, 44).

To calculate minimum paleodischarge, we surveyed a cross-section and long profile using a total station (Fig. 4 *A* and *C*). Sediment-size measurements of the intermediate particle axis (Fig. 4*B*) were made on a regular-spaced grid (Fig. 2*A*). Thalweg flow depths required for transport of the median particle size were calculated using ref. 45. Using calculated water depth and surveyed canyon cross-sectional area (Fig. 4*C*), we calculated the minimum paleoflood discharge following (46), where the bed-roughness length scale was 1.3 D_{84} (where D_{84} = 1.3 m is the sediment diameter in which 84% of the bed is finer; Fig. 4*B*) following a calibration in similar Box Canyon (19).

ACKNOWLEDGMENTS. We thank Joel Scheingross, Mathieu Lapotre, and Jim McKean for field assistance; Willy Amidon for sample preparation; and Bill Phillips for regional comparisons and mapping. This work was supported by NSF Grant 1147381 and NASA Grant PGG12-0107 to M.P.L. Comments from two reviewers strengthened the final version of this paper.

1. Whipple KX (2004) Bedrock rivers and the geomorphology of active orogens. *Annu Rev Earth Planet Sci* 32:151–185.
2. Berlin MM, Anderson RS (2007) Modeling of knickpoint retreat on the Roan Plateau, western Colorado. *J Geophys Res* 112(F3):1–16.
3. Laity JE, Malin MC (1985) Sapping processes and the development of theater-headed valley networks on the Colorado Plateau. *Geol Soc Am Bull* 96:203–217.
4. Sharp RP, Malin MC (1975) Channels on Mars. *Geol Soc Am Bull* 86(5):593–609.
5. Lamb MP, et al. (2006) Can springs cut canyons into rock? *J Geophys Res* 111(E7):1–18.
6. Malin MC, Carr MH (1999) Groundwater formation of martian valleys. *Nature* 397(6720):589–591.
7. Stearns HT (1936) Origin of the large springs and their alcoves along the Snake River in southern Idaho. *J Geol* 44:429–450.
8. Petroff AP, et al. (2011) Geometry of valley growth. *J Fluid Mech* 673:245–254.
9. Bandfield JL, Hamilton VE, Christensen PR (2000) A global view of Martian surface compositions from MGS-TES. *Science* 287(5458):1626–1630.
10. Milazzo MP, et al. (2009) Discovery of columnar jointing on Mars. *Geology* 37(2):171–174.
11. Warner NH, Gupta S, Kim J-R, Lin S-Y, Muller J-P (2010) Retreat of a giant cataract in a long-lived (3.7-2.6 Ga) martian outflow channel. *Geology* 38(9):791–794.
12. Craddock RA, Howard AD (2002) The case for rainfall on a warm, wet early Mars. *J Geophys Res* 107(E11):1–36.
13. Howard AD, McLane CF (1988) Erosion of cohesionless sediment by groundwater seepage. *Water Resour Res* 24(10):1659–1674.
14. Schumm SA, Boyd KF, Wolff CG, Spitz WJ (1995) A ground-water sapping landscape in the Florida Panhandle. *Geomorphology* 12(4):281–297.
15. Pelletier JD, Baker VR (2011) The role of weathering in the formation of bedrock valleys on Earth and Mars: A numerical modeling investigation. *J Geophys Res* 116(E11007):1–13.
16. Howard AD, Kochel RC, Holt H (1988) Sapping features of the Colorado Plateau: A comparative planetary geology field guide. *NASA Spec Publ* 491:71–83.
17. Haviv I, et al. (2010) Evolution of vertical knickpoints (waterfalls) with resistant caprock: Insights from numerical modeling. *J Geophys Res* 115:1–22.
18. Lamb MP, Dietrich WE (2009) The persistence of waterfalls in fractured rock. *Geol Soc Am Bull* 121(7–8):1123–1134.
19. Lamb MP, Dietrich WE, Aciego SM, Depaolo DJ, Manga M (2008) Formation of Box Canyon, Idaho, by megaflood: Implications for seepage erosion on Earth and Mars. *Science* 320(5879):1067–1070.
20. Bretz JH (1923) The channeled scabland of the Columbia Plateau. *J Geol* 31:617–649.
21. Malde HE (1968) The Catastrophic Late Pleistocene Bonneville Flood in the Snake River Plain, Idaho, *USGS Prof Pap*, 596:1–52.
22. Malde HE (1991) Quaternary geology and structural history of the Snake River Plain, Idaho and Oregon. *Quaternary Nonglacial Geology; Conterminous U.S*, ed Morrison RB (Geol Soc Am, Boulder, CO), Vol K-2, pp 251–280.
23. Kauffman JD, Otherberg KL, Gillerman VS, Garwood DL (2005) *Geologic Map of the Twin Falls 30 x 60 Minute Quadrangle, Idaho* (Idaho Geol Surv, Moscow, ID).
24. Malde HE (1971) History of the Snake River canyon indicated by revised stratigraphy of the Snake River Group near Hagerman and King Hill, Idaho. *US Geol Surv Prof Pap 644-F*, 20 pp.
25. Tauxe L, Luskin C, Selkin P, Gans P, Calvert A (2004) Paleomagnetic results from the Snake River Plain: Contribution to the time-averaged field global database. *Geochem Geophys Geosyst* 5(8):1–19.
26. Aciego SM, et al. (2007) Combining He-3 cosmogenic dating with U-Th/He eruption ages using olivine in basalt. *Earth Planet Sci Lett* 254(3–4):288–302.
27. Miller DM, Oviatt CG, McGeehin JP (2013) Stratigraphy and chronology of Provo shoreline deposits and lake-level implications, Late Pleistocene Lake Bonneville, eastern Great Basin, USA. *Boreas* 42(2):342–361.
28. Amidon WH, Clark A, Barrett B (2011) Snake River side canyons: Ages and process of formation. *The Bonneville Flood Revisited*, ed Crosby BT (Friends of the Pleistocene Guidebook), pp 50–61. Available at http://www2.cose.isu.edu/~crosby/fop_flood/FOP2011_Bonneville_Flood.pdf. Accessed June 1, 2013.
29. Goodman NM, Bray JW (1977) Toppling of rock slopes. *Rock Engineering for Foundations and Slopes* (Am Soc Civ Eng, NY), pp 201–234.
30. O'Connor JE (1993) *Hydrology, Hydraulics and Geomorphology of the Bonneville Flood* (Geol Soc Am, Boulder, CO), 90 pp.
31. Forman SL, Smith RP, Hackett WR, Tullis JA, McDaniel PA (1993) Timing of late Quaternary glaciations in the western United States based on the age of loess on the eastern Snake River Plain, Idaho. *Quat Res* 40(1):30–37.
32. Sims KWW, et al. (2007) Determining eruption ages and erosion rates of Quaternary basaltic volcanism from combined U-series disequilibria and cosmogenic exposure ages. *Geology* 35(5):471–474.
33. Rathburn SL (1993) Pleistocene cataclysmic flooding along the Big Lost River, east central Idaho. *Geomorphology* 8(4):305–319.
34. Cerling TE, Poreda RJ, Rathburn SL (1994) Cosmogenic He-3 and Ne-21 age of the Big Lost River Flood, Snake River Plain, Idaho. *Geology* 22(3):227–230.
35. Tomasson H (1973) Hamfarahlaup i Jokulsa a Fjollum. *Natturufraeoingurinn* 43:12–34.
36. Warner NH, Sowe M, Gupta S, Dumke A, Goddard K (2013) Fill and spill of giant lakes in the eastern Valles Marineris region of Mars. *Geology* 41(6):675–678.
37. Luo W, Howard AD (2008) Computer simulation of the role of groundwater seepage in forming Martian valley networks. *J Geophys Res* 113(E5):1–14.
38. Kurz MD (1986) In-situ production of terrestrial cosmogenic helium and some applications in geochronology. *Geochim Cosmochim Acta* 50(12):2855–2862.
39. Amidon WH, Farley KA (2011) Cosmogenic He-3 production rates in apatite, zircon and pyroxene inferred from Bonneville flood erosional surfaces. *Quat Geochronol* 6(1):10–21.
40. Cerling TE, Craig H (1994) Geomorphology and in-situ cosmogenic isotopes. *Annu Rev Earth Planet Sci* 22:273–317.
41. Lifton NA, et al. (2005) Addressing solar modulation and long-term uncertainties in scaling secondary cosmic rays for in situ cosmogenic nuclide applications. *Earth Planet Sci Lett* 239(1–2):140–161.
42. Sato T, Niita K (2006) Analytical functions to predict cosmic-ray neutron spectra in the atmosphere. *Radiat Res* 166(3):544–555.
43. Balco G, Stone JO, Lifton NA, Dunai TJ (2008) A complete and easily accessible means of calculating surface exposure ages or erosion rates from (10)Be and (26)Al measurements. *Quat Geochronol* 3(3):174–195.
44. Goehring BM, et al. (2010) A reevaluation of in situ cosmogenic He-3 production rates. *Quat Geochronol* 5:410–418.
45. Lamb MP, Dietrich WE, Venditti JG (2008) Is the critical Shields stress for incipient sediment motion dependent on channel-bed slope? *J Geophys Res* 113(F2):1–20.
46. Bathurst JC (2002) At-a-site variation and minimum flow resistance for mountain rivers. *J Hydrol* 269(1–2):11–26.

Supporting Information

Lamb et al. 10.1073/pnas.1312251111

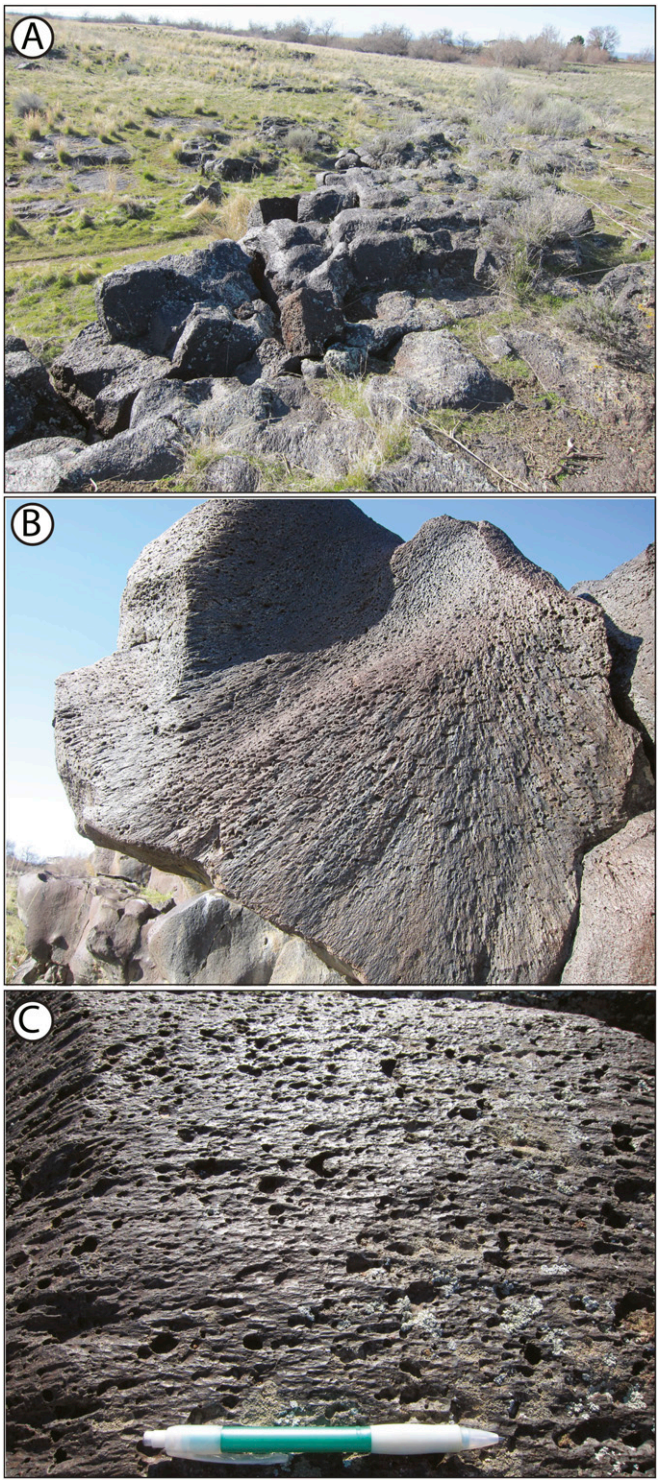

Fig. S1. Examples of scoured rock near the abandoned channel on the north side of Stubby Canyon (Fig. 2*B*). (*A*) Abraded and fluted bedrock where large-scale rock roughness in the foreground is ~1 m. (*B*) Close-up of abraded rock (~1 m in diameter) from *A* showing curvature of fine-scale flutes. (*C*) Close up photograph of fluted rock from *B* showing centimeter-scale flutes that fan out in the inferred flow direction (left to right). (Pencil for scale, 15 cm.)

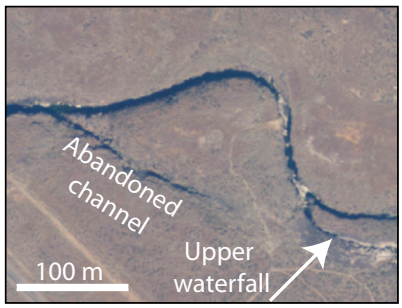

Fig. S2. Aerial orthophoto of the upstream extent of the knickzone in Pointed Canyon showing the most upstream waterfall (Fig. 3*E* and black circle in Fig. 2*B*) and the most upstream abandoned channel (Fig. 3*F* and blue dashed line in Fig. 2*B*) (US Geological Survey).

Table S1. Geochemical measurements

Sample name	Olivine mass (g)	$[^3He]_{melt}$ (10^6 at/g)	$[^4He]_{melt}$ (10^{12} at/g)	$(^3He/^4He)_{melt}$ (R/R_A)	Topographic shielding factor	$[^3He]_{cosmo}$ (10^6 at/g)	Production rate ($at^{-1} \cdot g^{-1} \cdot y^{-1}$)
GB0	0.1175	0.38 ± 0.02	0.33 ± 0.02	0.83	0	—	
MB0	0.4262	0.06 ± 0.01	0.24 ± 0.01	0.19	0	—	
NB0	0.3534	0.26 ± 0.02	0.12 ± 0.01	1.60	0	—	
S1	0.166	11.9 ± 0.71	0.62 ± 0.03	13.7	0.95	11.5 ± 0.75	246
S2	0.2532	5.60 ± 0.34	0.96 ± 0.05	4.17	0.96	5.2 ± 0.34	250
S3	0.17	4.77 ± 0.29	0.44 ± 0.02	7.72	0.98	4.4 ± 0.28	255
S4	0.0937	4.73 ± 0.28	5.87 ± 0.3	0.58	0.91	4.3 ± 0.28	237
S5	0.1765	6.01 ± 0.36	17.4 ± 0.9	0.25	0.93	5.6 ± 0.36	243
W1	0.1179	12.5 ± 0.75	1.75 ± 0.1	5.10	1.00	12.1 ± 0.79	254
P1	0.306	5.63 ± 0.34	1.14 ± 0.06	3.54	0.98	5.3 ± 0.34	255
P2	0.1716	7.62 ± 0.46	0.40 ± 0.02	13.6	0.86	7.2 ± 0.47	225
P3	0.3901	3.16 ± 0.19	0.15 ± 0.01	15.5	1.00	2.8 ± 0.18	260
P4	0.3849	5.40 ± 0.32	0.12 ± 0.01	32.1	1.00	5.0 ± 0.32	261
P5	0.1213	4.82 ± 0.29	1.10 ± 0.05	3.13	0.99	4.4 ± 0.29	254
P6	0.0379	6.05 ± 0.36	196 ± 10	0.02	0.85	5.7 ± 0.37	219
MB1	0.1121	8.21 ± 0.50	1.35 ± 0.07	4.36	0.98	8.1 ± 0.53	257
NB1	0.359	15.1 ± 0.90	0.24 ± 0.01	44.2	1.00	14.9 ± 0.97	279

Samples GB0, MB0, and NB0 are shielded samples for Gooding Butte Basalt (used to correct all canyon erosion data), McKinney Butte Basalt (used to correct McKinney Butte Basalt age: MB1), and Notch Butte Basalt (used to correct Notch Butte Basalt age: NB1). Subscript "melt" is helium released by heating powdered olivine under vacuum. $[^3He]_{cosmo}$ is cosmogenic ^3He after subtracting the shielded component (^3He measured in relevant shielded sample). R_A is the atmospheric $^3He/^4He$ isotope ratio of 1.4×10^{-6} and at denotes atoms. Basalt had a bulk density of 2.8 ± 0.1 g/cm^3. Error represents ±1 SD. Production rate was calculated using the Lifton/Sato scaling scheme (1, 2) on the CRONUS ^3He calculator (3, 4). Uncertainty in the shielded sample affects the absolute age but does not change relative ages between canyon heads or calculated knickpoint retreat rates.

1. Lifton NA, et al. (2005) Addressing solar modulation and long-term uncertainties in scaling secondary cosmic rays for in situ cosmogenic nuclide applications. *Earth Planet Sci Lett* 239(1–2):140–161.
2. Sato T, Niita K (2006) Analytical functions to predict cosmic-ray neutron spectra in the atmosphere. *Radiat Res* 166(3):544–555.
3. Balco G, Stone JO, Lifton NA, Dunai TJ (2008) A complete and easily accessible means of calculating surface exposure ages or erosion rates from (10)Be and (26)Al measurements. *Quat Geochronol* 3(3):174–195.
4. Goehring BM, et al. (2010) A reevaluation of in situ cosmogenic He-3 production rates. *Quat Geochronol* 5:410–418.

Table S2. Sample locations and exposure ages

Sample	Canyon	Description	Latitude (°)	Longitude (°)	Elevation (m)	Age (ka)
S1	Stubby	Rim notch	42.8677	−114.863	983	46.2 ± 2.9
S2	Stubby	Rim notch	42.86765	−114.863	991	21.6 ± 1.3
S3	Stubby	Rim notch	42.86766	−114.863	990	18.0 ± 1.1
S4	Stubby	Side rim notch	42.86755	−114.866	992	19.1 ± 1.1
S5	Stubby	Side rim notch	42.86758	−114.866	993	23.8 ± 1.4
W1	Woody	Rim notch	42.85423	−114.881	972	47.2 ± 3.0
P1	Pointed	Abandoned channel	42.86739	−114.859	991	21.2 ± 1.2
P2	Pointed	Abandoned channel	42.8682	−114.858	995	32.5 ± 1.9
P3	Pointed	Strath terrace	42.86777	−114.85	990	11.3 ± 0.7
P4	Pointed	Abandoned channel	42.86727	−114.849	993	19.9 ± 1.1
P5	Pointed	Strath terrace	42.86798	−114.851	984	18.2 ± 1.0
P6	Pointed	Strath terrace	42.86783	−114.854	981	26.3 ± 1.5
MB1	McKinny Butte flow top		42.89116	−114.918	978	31.9 ± 1.9
NB1	Notch Butte flow top		42.82378	−114.706	1074	52.8 ± 3.4

Exposure ages were calculated using the CRONUS 3He Exposure Calculator (1, 2) using the Lifton/Sato scaling scheme (3, 4) (see production rate in Table S1). Error on age represents 1 SD of external uncertainty as determined by the exposure age calculator.

1. Balco G, Stone JO, Lifton NA, Dunai TJ (2008) A complete and easily accessible means of calculating surface exposure ages or erosion rates from (10)Be and (26)Al measurements. *Quat Geochronol* 3(3):174–195.
2. Goehring BM, et al. (2010) A reevaluation of in situ cosmogenic He-3 production rates. *Quat Geochronol* 5:410–418.
3. Lifton NA, et al. (2005) Addressing solar modulation and long-term uncertainties in scaling secondary cosmic rays for in situ cosmogenic nuclide applications. *Earth Planet Sci Lett* 239(1–2):140–161.
4. Sato T, Niita K (2006) Analytical functions to predict cosmic-ray neutron spectra in the atmosphere. *Radiat Res* 166(3):544–555.